Electronic Supplementary Information

Polyelectrolyte Complex-Based Self-Healing, Fatigue-Resistant and Anti-Freezing Hydrogels as Highly Sensitive Ionic Skins

Siheng Li, Hongyu Pan, Yuting Wang and Junqi Sun*

State Key Laboratory of Supramolecular Structure and Materials, College of Chemistry, Jilin University, Changchun 130012, People's Republic of China

*Corresponding authors. E-mail: sun_junqi@jlu.edu.cn

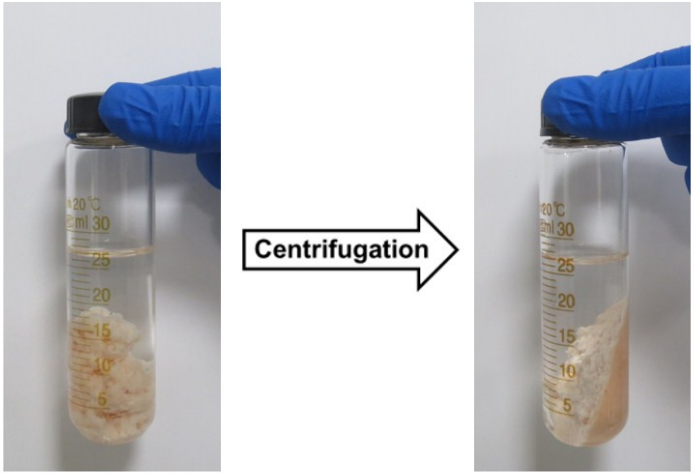

Fig. S1 Photos of the PAAm/PAA-1.1%Fe^{3+} complexes before and after centrifugation.

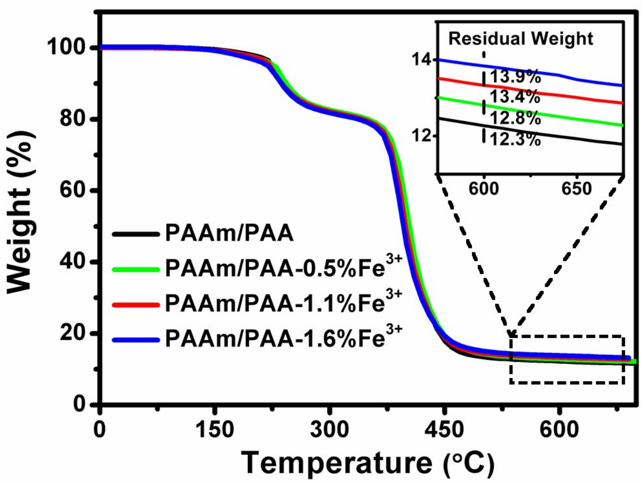

Fig. S2 TGA curves of the PAAm/PAA and PAAm/PAA-x%Fe^{3+} xerogels with different mass fraction of $FeCl_3$.

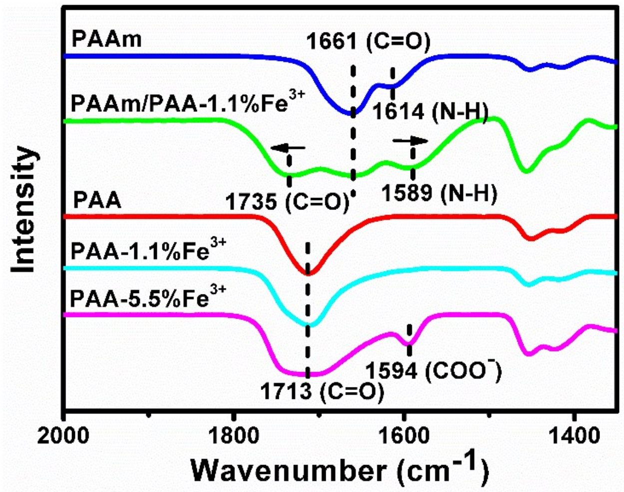

Fig. S3 FT-IR spectra of the PAAm, PAA, PAA-1.1%Fe^{3+} and PAA-5.5%Fe^{3+} films and PAAm/PAA-1.1%Fe^{3+} composite in the range of 2000 to 1380 cm^{-1}.

FT-IR spectra of pure PAAm, PAA, PAA-1.1%Fe^{3+}, and PAA-5.5%Fe^{3+} casting films and the PAAm/PAA-1.1%Fe^{3+} composites are shown in Fig. S3. The characteristic peak at 1713 cm^{-1} in the PAA casting film is attributed to the –C=O stretching vibration of the carboxylic acid groups in PAA. The FT-IR spectrum of the PAA-1.1%Fe^{3+} film shows no obvious changes compared with that of pure PAA film. However, the spectrum of PAA-5.5%Fe^{3+} casting film shows a new characteristic peak at 1594 cm^{-1}, which is assigned to the carboxylate groups of PAA coordinated with Fe^{3+} ions. The characteristic peak of the carbonyl groups of carboxylic acid groups in PAA shifts from 1713 to 1735 cm^{-1} in the PAAm/PAA-1.1%Fe^{3+} composites. Meanwhile, the characteristic peak of the amide groups in PAAm film at 1614 cm^{-1} shifts to 1589 cm^{-1} in the PAAm/PAA-1.1%Fe^{3+} composites. These shifts of the carbonyl and amide groups in the FT-IR spectra prove the existence of hydrogen-bonding interactions between carboxylic acid groups of PAA and amide groups of PAAm in the PAAm/PAA-1.1%Fe^{3+} composites. Therefore, the coordination interactions between PAA and Fe^{3+} ions and the hydrogen-bonding interactions between PAAm and PAA are the primary driving forces for the formation of the PAAm/PAA-1.1%Fe^{3+} hydrogels.

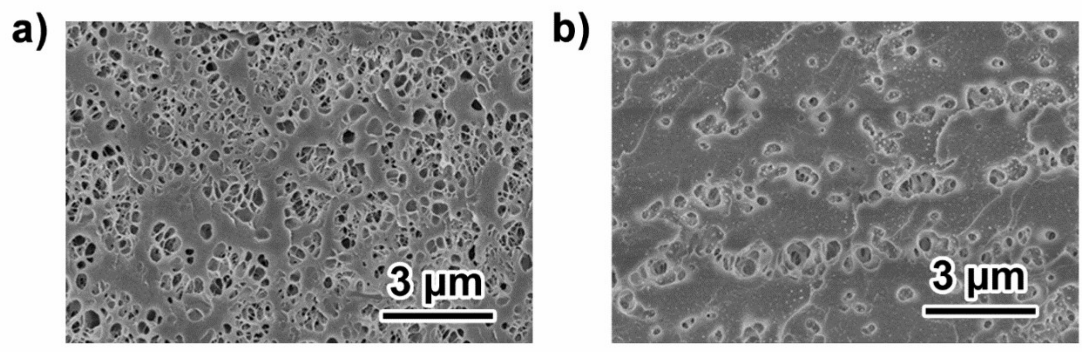

Fig. S4 Cross-sectional SEM images of the PAAm/PAA-1.1%Fe^{3+} (a) and PAAm/PAA-1.1%Fe^{3+}/NaCl (b) hydrogels.

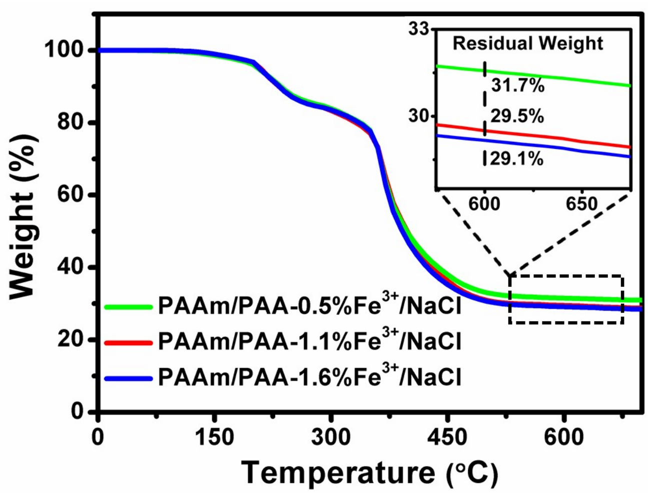

Fig. S5 TGA curves of the PAAm/PAA-x%Fe^{3+}/NaCl xerogels with different mass fraction of $FeCl_3$.

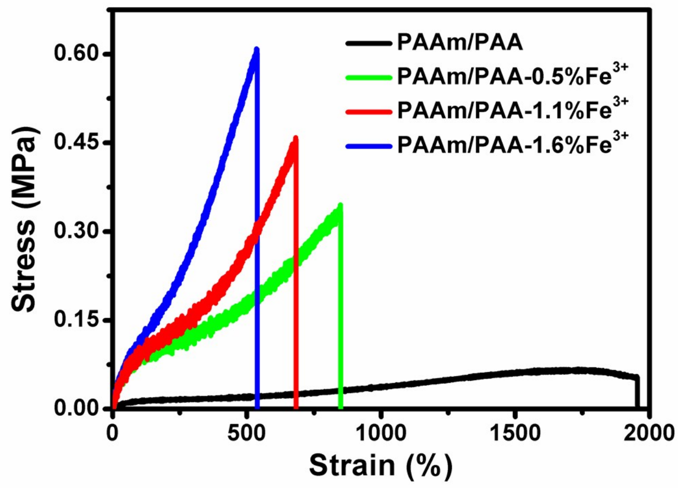

Fig. S6 Stress-strain curves of the PAAm/PAA and the PAAm/PAA-x%Fe^{3+} hydrogels.

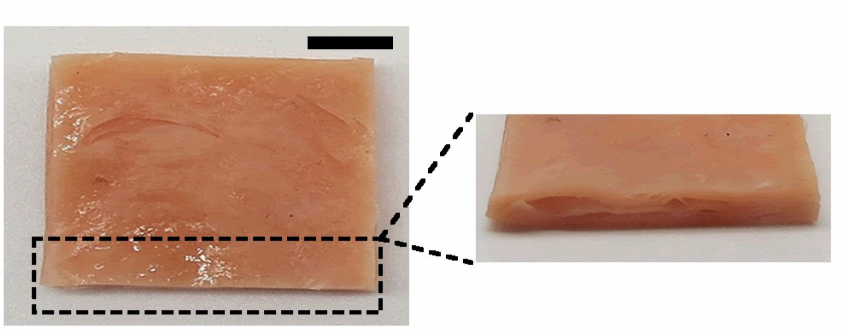

Fig. S7 Digital photographs of the PAAm/PAA-1.6%Fe^{3+}/NaCl hydrogel. The scale bar is 1 cm.

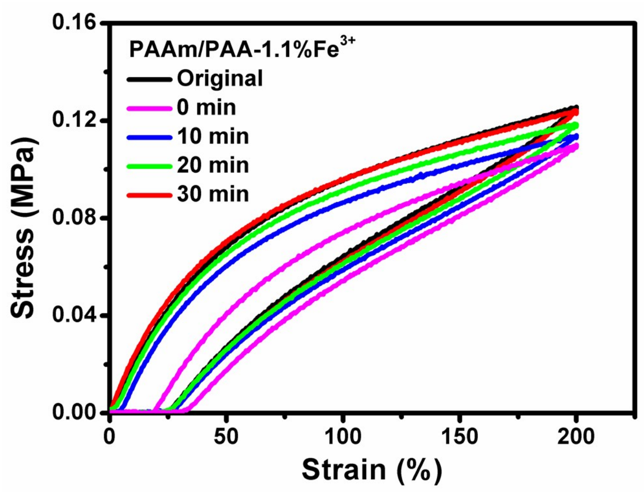

Fig. S8 Stress-strain curves of the PAAm/PAA-1.1%Fe^{3+} hydrogels measured via cyclic tensile tests with different rest time between each stretch−release cycle.

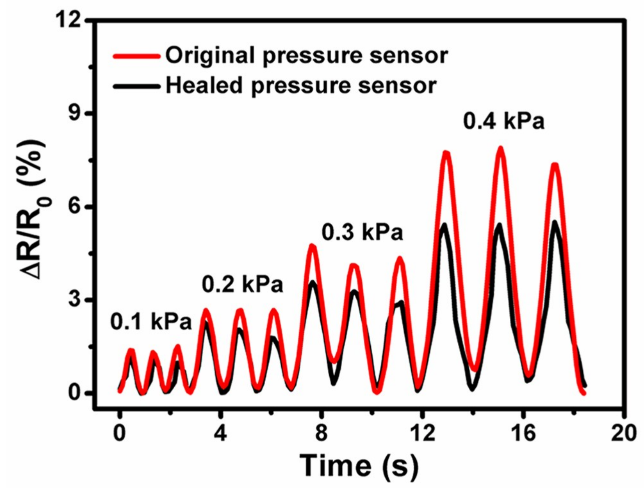

Fig. S9 Relative resistance changes of the hydrogel-based ionic skins after different cycles of weak pressure measurements (0.1 kPa, 0.2 kPa, 0.3 kPa, 0.4 kPa).

Table S1. Comparison of comprehensive performances of the hydrogel-based sensors.

Type	Components	Tensile Stress (kPa)	Tensile Strain (%)	Modulus (kPa)	Gauge Factor	Sensitivity (kPa^{-1})	Detection Limit		Anti-freezing Property	Self-healing Property	Ref.
							Strain (%)	Pressure (kPa)			
HI[a]	**PAAm/PAA/$FeCl_3$/NaCl**	**1180**	**573**	**330**	**1.96**	**0.75**	**0.2-500**	**0.1-10**	**Yes**	**Yes**	**This work**
HI	PVA/TA@talc/$AlCl_3$/EG	650	700	N/A	1.3	N/A	100	N/A	Yes	N/A	[1]
HI	PVA/PAAm/KCl	180	500	87	N/A	0.05	N/A	7	N/A	N/A	[2]
HI	PAM/LiCl/PDMS	N/A	50	N/A	0.84	N/A	50	N/A	N/A	N/A	[3]
HI	PAAm/SA/NaCl	650	2000	50	2.66	1.45	0.3-1800	0.1-6	N/A	Yes	[4]
HI	PAA/PDMAPS/NaCl	N/A	10000	28	N/A	N/A	100	N/A	N/A	Yes	[5]
HI	PAA/TA@CNC/$AlCl_3$	300	2800	80	7.8	N/A	2000	N/A	N/A	Yes	[6]
HI	ACC/PAA/SA	6	1000	6.7	N/A	0.17	N/A	1	N/A	Yes	[7]
HI	PAAm/SA/TA	50	4000	8	2	N/A	0.05-2100	N/A	N/A	Yes	[8]
HI	KCl/κ-Carrageenan/PAM	575	2000	120	0.63	N/A	1000	N/A	N/A	Yes	[9]
HI	P(AAM-HMA)/AMP/CTMAB/NaCl	620	2160	25	2.37	N/A	1000	N/A	N/A	N/A	[10]
HI	PAM/NaCl	N/A	600	N/A	N/A	N/A	500	40	N/A	N/A	[11]
HI	PSBMA/PHEMA/Laponite	270	2000	N/A	1.8	N/A	100	N/A	N/A	Yes	[12]
HI	PDA-talc/PAM/KCl	15	1500	80	N/A	N/A	1000	N/A	N/A	Yes	[13]

HI	PVA/GE/Glycerin/NaCl	1040	715	157	0.74	N/A	700	N/A	Yes	N/A	[14]
HE[b]	PVA/FSWCNT/PDA	N/A	N/A	＜10	N/A	N/A	N/A	N/A	N/A	Yes	[15]
HE	PVA/PAA/CNT/$FeCl_3$/PEDOT-PSS/EG	28.33	550	N/A	1.6	0.243	100	25	Yes	Yes	[16]
HE	PAA/GO/$CaCl_2$	750	2500	N/A	N/A	N/A	N/A	N/A	N/A	Yes	[17]
HE	PVA/SWCNT	N/A	N/A	＜10	1.51	N/A	1000	N/A	N/A	Yes	[18]
HE	PANI/P(AAm-co-HEMA)	1520	310	N/A	1.48	N/A	300	N/A	N/A	N/A	[19]
HE	PANI/PSS–UPy	N/A	N/A	＜3	3.4	N/A	300	N/A	N/A	Yes	[20]
HE	PDA-PPy/PAAM	90	1600	N/A	N/A	N/A	N/A	N/A	N/A	N/A	[21]

[a,b] HI and HE are donated as “hydrogel-based ionic skin sensors“ and “hydrogel-based electronic skin sensors“, respectively.

N/A is donated as “not available“ in the references.

References

1. X. Pan, Q. Wang, R. Guo, Y. Ni, K. Liu, X. Ouyang, L. Chen, L. Huang, S. Cao and M. Xie, *J. Mater. Chem. A*, 2019, **7**, 4525-4535.
2. G. Ge, Y. Zhang, J. Shao, W. Wang, W. Si, W. Huang and X. Dong, *Adv. Funct. Mater.*, 2018, **28**, 1802576.
3. K. Tian, J. Bae, S. E. Bakarich, C. Yang, R. D. Gately, G. M. Spinks, M. i. H. Panhuis, Z. Suo and J. J. Vlassak, *Adv. Mater.*, 2017, **29**, 1604827.
4. X. Zhang, N. Sheng, L. Wang, Y. Tan, C. Liu, Y. Xia, Z. Nie and K. Sui, *Mater. Horiz.*, 2019, **6**, 326-333.
5. Z. Lei and P. Wu, *Nat. Commun.*, 2018, **9**, 1134.
6. C. Shao, M. Wang, L. Meng, H. Chang, B. Wang, F. Xu, J. Yang and P. Wan, *Chem. Mater.*, 2018, **30**, 3110-3121.
7. Z. Lei, Q. Wang, S. Sun, W. Zhu and P. Wu, *Adv. Mater.*, 2017, **29**, 1700321.
8. H. Qiao, P. Qi, X. Zhang, L. Wang, Y. Tan, Z. Luan, Y. Xia, Y. Li and K. Sui, *ACS Appl. Mater. Interfaces*, 2019, **11**, 7755-7763.
9. S. Liu and L. Li, *ACS Appl. Mater. Interfaces*, 2017, **9**, 26429-26437.
10. Q. Zhang, X. Liu, X. Ren, F. Jia, L. Duan and G. Gao, *Chem. Mater.*, 2019, **31**, 5881-5889.
11. J. Y. Sun, C. Keplinger, G. M. Whitesides and Z. Suo, *Adv. Mater.*, 2014, **26**, 7608-7614.
12. L. Wang, G. Gao, Y. Zhou, T. Xu, J. Chen, R. Wang, R. Zhang and J. Fu, *ACS Appl. Mater. Interfaces*, 2019, **11**, 3506-3515.

13. X. Jing, H.-Y. Mi, Y.-J. Lin, E. Enriquez, X.-F. Peng and L.-S. Turng, *ACS Appl. Mater. Interfaces*, 2018, **10**, 20897-20909.

14. H. Chen, X. Ren and G. Gao, *ACS Appl. Mater. Interfaces*, 2019, **11**, 28336-28344.

15. M. Liao, P. Wan, J. Wen, M. Gong, X. Wu, Y. Wang, R. Shi and L. Zhang, *Adv. Funct. Mater.*, 2017, **27**, 1703852.

16. G. Ge, W. Yuan, W. Zhao, Y. Lu, Y. Zhang, W. Wang, P. Chen, W. Huang, W. Si and X. Dong, *J. Mater. Chem. A*, 2019, **7**, 5949-5956.

17. Y. Wang, Q. Chang, R. Zhan, K. Xu, Y. Wang, X. Zhang, B. Li, G. Luo, M. Xing and W. Zhong, *J. Mater. Chem. A*, 2019, **7**, 24814-24829.

18. G. Cai, J. Wang, K. Qian, J. Chen, S. Li and P. S. Lee, *Adv. Sci.*, 2017, **4**, 1600190.

19. Z. Wang, J. Chen, Y. Cong, H. Zhang, T. Xu, L. Nie and J. Fu, *Chem. Mater.*, 2018, **30**, 8062-8069.

20. J. Chen, Q. Peng, T. Thundat and H. Zeng, *Chem. Mater.*, 2019, **31**, 4553-4563.

21. L. Han, L. Yan, M. Wang, K. Wang, L. Fang, J. Zhou, J. Fang, F. Ren and X. Lu, *Chem. Mater.*, 2018, **30**, 5561-5572.